A Model of the Interfacial Heat-Transfer Coefficient during Unidirectional Solidification of an Aluminum Alloy

W.D. GRIFFITHS

A model is presented for the prediction of the interfacial heat-transfer coefficient during the unidirectional solidification vertically upward of an Al-7 wt pct Si alloy cast onto a water cooled copper chill. It has been experimentally determined that the casting surfaces were convex toward the chill, probably due to the deformation of the initial solidified skin of the casting. The model was, therefore, based upon a determination of the (macroscopic) nominal contact area between the respective rough surfaces and, within this region, the actual (microscopic) contact between the casting and the chill surfaces. The model produced approximate agreement with both experimentally determined values of the heat-transfer coefficient and the measured curvature of the casting surface and showed a reasonable agreement with measured temperatures in the casting and the chill also. A common experimental technique for the experimental determination of the heat-transfer coefficient involves the assumption of one-dimensional heat transfer only. An implication of the approach adopted in this model is that the heat transfer in the region of the casting-chill interface may be two-dimensional, and the subsequent error in the experimentally determined values is discussed.

I. INTRODUCTION

THE production of castings has been greatly assisted by the development of models of their solidification. These models require a knowledge of the thermophysical properties of the solidifying alloy and of the heat transfer between the casting and its mold. In the latter case, many experiments have been carried out to measure the interfacial heat-transfer coefficient for simple castings solidifying unidirectionally against a chill. These have shown that the values obtained can differ greatly and are dependent on many variables of the casting process. Particularly important factors appear to be the application of pressure (for example, in squeeze casting), the orientation of the casting-mold interface with respect to gravity (which would also have a strong influence on the pressure between the casting and the mould surfaces at their interface), and the presence or absence of mould coatings. The influence of many other factors (alloy superheat, composition, liquid alloy surface tension, mould or chill preheat, *etc.*) has also been recognized. The heat-transfer coefficients measured in the unidirectionally solidified experiments can, therefore, only be used as a guide in casting solidification modeling. Alternatively, if the actual processes that influence the heat transfer at the casting-mold interface could be modeled, then the interfacial heat-transfer coefficient could be predicted as part of the progress of the casting solidification model itself.

The mechanisms by which heat is transferred through the interface between a casting as it solidified against a metal chill (to represent a die) have been the subject of detailed investigation by Ho and Pehlke[1,2] and Pehlke.[3] They suggested that, initially, a thin skin of solidified metal formed in contact with the chill surface, and that heat transfer occurred by conduction through the peaks of the rough surfaces of the casting and the chill in contact, and also by conduction through the atmosphere contained in the voids between the contact areas. As solidifcation progressed the relative expansion and contraction of the chill and the casting altered the amount of contact and the size of the interfacial gap between the two surfaces. Eventually this led to their complete separation. In this case the heat transfer coefficient was greatly reduced as heat was extracted from the casting through a relatively insulating "air gap."

Relatively low melting point alloys, such as aluminum, were studied, so radiation made a negligible contribution to the heat-transfer process. Furthermore, the gap between the casting and the chill surfaces was sufficiently small so convection was not thought to have occurred. The authors pointed out that, while it is often convenient to assume that the atmosphere in the interfacial region is air, it may also, of course, contain other gases with differing thermal conductivities.

Several quantitative models of the heat-transfer coefficient during casting solidification have been developed based on this idea of an initial contact stage, in which the casting is in close contact with the die or chill surface, followed by a stage in which an air gap formed. However, these models are mostly concerned with the development of the air gap rather than with the prior contact stage. For example, Nishida *et al.*, in 1986,[4] modeled the formation of the air gap using an analytical elastic model for predicting the movement of the mold wall relative to the casting surface. Trovant and Argyropolis[5] recently produced a numerical elastic model of a casting to predict air-gap formation. Several models for predicting the air gap but involving only a consideration of the thermal contraction of the casting have also been presented.[6,7,8] In addition, Shahverdi *et al.*[9] predicted the air gap formation in the case of a casting in a sand mold. More detailed thermomechanical models of the casting solidification process using the finite element method have been carried out, and some have incorporated a prediction of the

W.D. GRIFFITHS, Federal-Mogul Senior Research Fellow, is with the Manchester Materials Science Centre, University of Manchester and UMIST, Manchester, United Kingdom M1 7HS.

Manuscript submitted November 10, 1998.

air gap to predict the heat-transfer coefficient as part of the model.[10,11]

In related work, Sharma and Krishnan[12] considered the initial period of contact of the cast liquid alloy with the die surface, and modeled the heat-transfer coefficient associated with penetration of the liquid alloy into the valleys of the roughness of the surface upon which it rested.

Models have also been proposed in which the individual thermal resistances at the casting-mold interface have been examined in detail for particular casting situations. For example, Mathew *et al.*[13] analyzed the heat-transfer resistances relevant to the solidification of lead against the base of a stainless steel container, and Chiesa[14] proposed a model of heat transfer through a coated die surface with the model being constructed from the separate thermal resistances of the die/coating/casting interface.

However, the qualitative model of Ho and Pehlke[2] is not the only explanation of interfacial heat transfer that has been put forward. For example, Svensson and Schmidt have proposed a model of heat transfer through an entrapped film of gas occurring between the liquid metal and the die surface.[15]

Another alternative view of the mechanisms that govern heat transfer at a casting-chill interface was advanced by Griffiths[16,17] and Kayikci and Griffiths.[18] In their experiments, the surfaces of Al alloy castings, unidirectionally solidified against a plane Cu chill, were found to be convex toward the chill by amounts of around 10 to 20 μm. The convexity of the casting surface was thought to have been caused by the deformation of the solidifying skin of the casting soon after its formation, as proposed by Niyama and co-workers.[19,20] (A detailed model of this process has been reported by Thomas and Parkman[21]). Since the deformation probably occurred early in the casting process, perhaps even during pouring, it was suggested that it would have a significant effect on the subsequent heat transfer through the casting-chill interface.[17] This deformation of the initial solidified casting skin may have occurred in many of the previously reported measurements of the interfacial heat-transfer coefficient and may occur in many commonly used casting processes.

A model of the development of the heat-transfer coefficient with time for the experiment in which the deformation effect was observed (unidirectional solidification of Al-7 wt pct Si alloy against a Cu chill[17]) has been developed and is reported here. The model includes the heat transfer through the actual contact area between a plane chill surface and a spherical casting surface and the heat transfer through the voids between, but also takes into account the local separation of the casting and the chill surfaces at the circumference of the interface caused by the deformation of the initial casting skin.

This approach, in conjunction with the models concentrating on the formation of the air gap, is an important step toward the development of a predictive model of the interfacial heat-transfer coefficient during casting solidification.

II. THE EXPERIMENTAL DETERMINATION OF THE HEAT-TRANSFER COEFFICIENT

The heat-transfer coefficient during unidirectional solidification was determined using the following experimental procedure. This has been described elsewhere in more detail[17] but is also briefly given here.

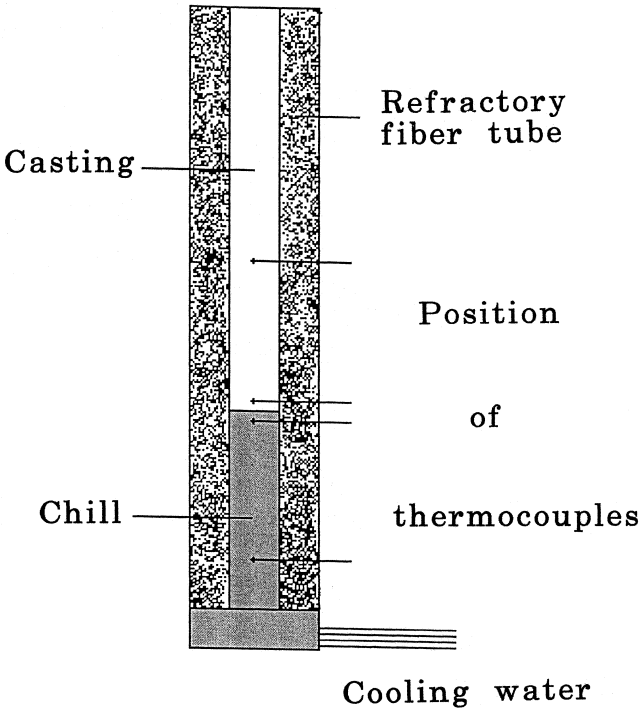

Fig. 1—Sketch of the experimental arrangement used to determine the interfacial heat-transfer coefficient during the unidirectional solidification of Al-7 wt pct Si alloys vertically upward.

An alloy of Al-7 wt pct Si was cast into a cylindrical refractory mold into the bottom of which was inserted a water cooled Cu chill (of 100 mm length) to induce unidirectional solidification. The refractory tubes were preheated to 900°C and allowed to cool before use in the experiment to eliminate the production of any volatile gases during the pouring and subsequent cooling of the casting. This should have ensured that the atmosphere of the interface between the casting and the chill was air, as assumed in the model. Before casting, the surface of the Cu chill was prepared using 240 grade SiC paper to obtain a reproducible surface finish. The casting dimensions were 200 mm in length and 25 mm in diameter, and four castings were made, each poured at a temperature of 780°C. The experimental arrangement was such that solidification took place vertically upward, as shown in Figure 1.

The surface finish parameters of the chill and casting surfaces were measured using an RS Surtronic 200 surface profileometer and are shown in Table I. In addition to surface

Table I. Measured Surface Roughness Data Obtained from the Chill and Casting Surfaces at their Interface*

Surface	R_a (μm)	R_z (μm)	S_m (μm)	R (m)
Chill	0.88	6.1	60.8	plane
Casting	1.50	9.8	140	6.9

*R_a is the arithmetic mean deviation of the surface profile, R_z is the mean peak-to-valley height measured in the traverse, while S_m is the mean distance between profile peaks. R is the radius of curvature of the surface.

roughness data, profiles were measured across the diameters of the castings and the chills resulting in the observation that the casting surfaces were not plane, but were convex toward the chill.[17] The mean radius of curvature of these surfaces is also shown in Table I.

The casting and the chill each contained thermocouples (Figure 1), which were read at intervals of 0.5 seconds by a computer controlled datalogger. The heat-transfer coefficients were calculated from this data by inversely solving the one-dimensional heat-transfer equation using an explicit finite difference method. Mean maximum values of the heat-transfer coefficient of 7.1 kW m^{-2} K^{-1}, in the case of upward solidification, were obtained.[17] As pointed out in Section I, these experimentally determined heat-transfer coefficients would be specific to these experimental conditions. However, they provided a case of solidification that was capable of being readily described and for which a simple model of the interfacial heat-transfer coefficient could be developed.

III. THE MODEL OF THE INTERFACIAL CONTACT AREA AND THE HEAT-TRANSFER COEFFICIENT DURING CASTING SOLIDIFICATION

The temperature distributions within the chill and the casting were calculated using an explicit one-dimensional finite difference model (Reference 22, for example) with a time-step of 0.001 seconds and a nodal distance of 1 mm in the chill and 2 mm in the casting. The number of elements used in the calculation was increased to show that the solution obtained was not sensitive to the selected nodal distance. Values of the thermophysical properties for both the chill and the casting, as well as other data used in the calculations, are shown in Table II.

The thermophysical property data for the alloy and the chill material were obtained from the published literature as indicated in the table. However, the estimated value of the thermal conductivity of the liquid alloy was increased by a factor of 3 to take into account the enhanced heat transfer in the bulk liquid alloy due to fluid flow arising from the pouring of the casting. This procedure has been found to improve the accuracy of the experimentally determined heat-transfer coefficients as shown, for example, in References 23 (in which a factor of about 8.5 was used) and 24 (a factor of 1.5). The latent heat evolved during solidification of the casting was incorporated into an effective specific heat capacity, as is explained elsewhere.[17]

The end of the casting away from the interface was assumed to be insulated while the boundary condition away from the interface in the chill (*i.e.*, the end of the chill in contact with the cooling water) was assumed to be described by a heat transfer coefficient given by a correlation for forced cooling:[22]

$$h_w = 0.023\mathrm{Re}^{0.8}\mathrm{Pr}^{0.3} \qquad [1]$$

The velocity of the cooling water in the base of the chill in this experiment was estimated to be 2.5 ms^{-1}.

A. *The Calculation of the Heat-Transfer Coefficient in the Initial Contact Stage*

Upon casting of the liquid alloy it was assumed that the liquid metal rested upon the chill surface and a solid skin immediately formed of negligible thickness but with a surface roughness as measured after the casting experiment was over. The initial temperature of the liquid alloy was assumed to be 727°C (1000 K), determined from the casting experiments, and the initial chill temperature was assumed to be 20°C (293 K). Any effects from oxide films occurring on the surface of the chill and on the liquid aluminum alloy were assumed to be negligible. Heat transfer due to conduction between the contact areas between the solid alloy and the chill surfaces was also assumed to be negligible for this short initial contact stage.

The heat transfer in the initial contact stage was, therefore, assumed to be by conduction alone from the thin solid casting skin to the cold chill surface through the interfacial atmosphere (assumed to be air). To determine the mean separation of the casting and chill surfaces, the surface roughnesses of both were combined into a sum surface roughness as follows;

$$R_{z(\Sigma)} = \sqrt{R^2_{z(\mathrm{chill})} + R^2_{z(\mathrm{casting})}} \qquad [2]$$

Here, the relevant parameter to describe the surface roughness was considered to be R_z, the mean peak-to-valley height measured within a traverse of the profileometer.[25] Surface roughness measurements of the prepared chill surface before casting, together with casting surface roughness data used in the model, are shown in Table I, and an explanation of the various surface parameters used in the model is shown schematically in Figure 2.

In moving from a gas to a solid surface, a discontinuity in temperature is observed. This has been described, by Kennard,[26] for example, using a "temperature jump coefficient," g, expressed in terms of the mean free path of the gas, λ. For example, g is equal to 2.7λ in the case of air. This

Table II. Physical Properties of the Cu Chill and Al-7 Wt Pct Si Alloy Used in the Model of the Heat-Transfer Coefficient*

Property (Units)	Value
Properties of copper	
Thermal conductivity (W m^{-1} K^{-1})	$416.51 - 0.05874\ T$
Specific heat capacity (J kg^{-1} K^{-1})	$351 + 0.11069$ T
Density (kg m^{-3})	$9095.11 - 0.4629\ T$
Coefficient of thermal expansion (K^{-1})	17.7×10^{-6}
Properties of Al-7 wt pct Si alloy (liquid)	
Thermal conductivity (W m^{-1} K^{-1})	88.6
Specific heat capacity (J kg^{-1} K^{-1})	1080
Density (kg m^{-3})	2394
Properties of Al-7 wt pct Si alloy (solid)	
Thermal conductivity (W m^{-1} K^{-1})	198
Specific heat capacity (J kg^{-1} K^{-1})	917
Density (kg m^{-3})	2672
Coefficient of thermal expansion (K^{-1})	24×10^{-6}
Characteristics of Al-7 wt pct Si alloy	
Latent heat (J kg^{-1})	397,490
Liquidus temperature (K)	890
Solidus (eutectic) temperature	850
Fraction solid of the primary phase	0.5248
Partition coefficient	0.13
Effective specific heat capacity	$3.415 \times 10^3 + 8.0234 \times 10^3\ T + 4.71754\ T^2$

*The physical properties of the Cu are expressed as a function of temperature (T) in Kelvin, while the physical properties of the alloy are assumed to be independent of temperature.

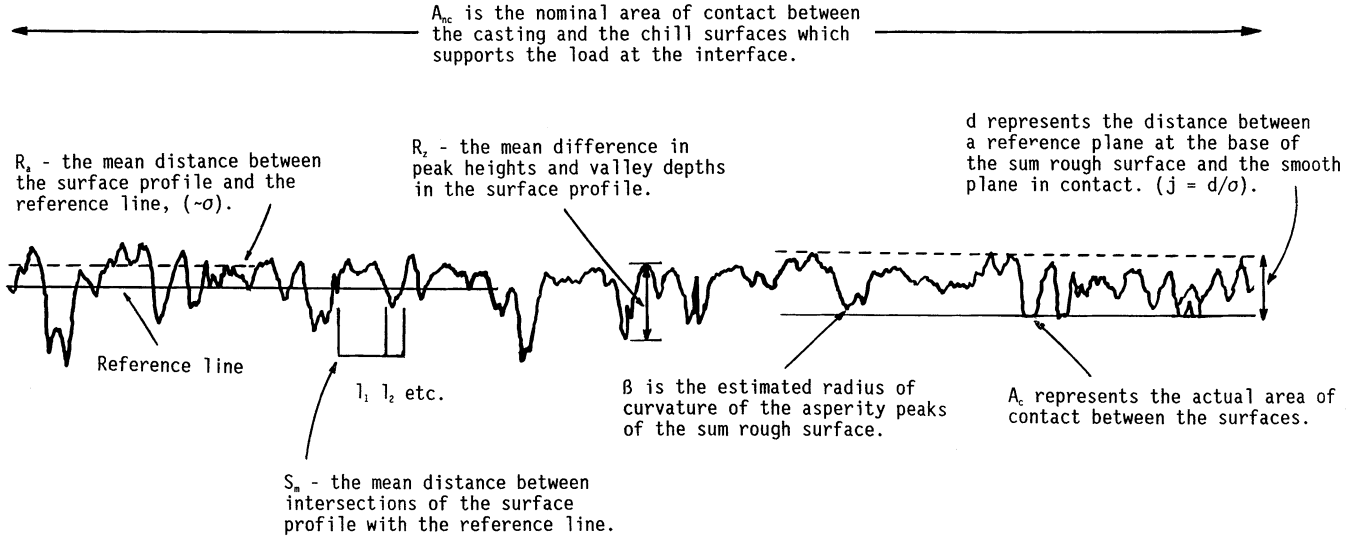

Fig. 2—Schematic to show the definitions of the surface roughness and other parameters used in the model of the chill-casting interface.

Table III. Physical Properties of Air, and Other Data, Used for the Calculation of the Temperature Jump Coefficient.[22]

Property (Units)	Value
Thermal conductivity (W m^{-1} K^{-1})	$-5.9958 \times 10^{-4} + 1.015 \times 10^{-4} T - 4.5616 \times 10^{-8} T^2 + 1.307 \times 10^{-11} T^3$
Density (kg m^{-3})	0.5879
Dynamic viscosity (kg m^{-1} s^{-1})	3.018×10^{-5}
Prandtl number	0.682
Ratio of specific heats	1.4
Boltzman's constant (J K^{-1})	1.23×10^{23}
Molecular mass	4.824×10^{-26}
Accommodation coefficient[26]	0.8

Table IV. The Mechanical Properties Used in the Model*

Property (Units)	Value
Alloy	
Yield stress (Pa)	$3.41 \times 10^9 \times 10^{-0.00383T}$
Youngs modulus (Pa)	71.0×10^9
Poisson's ratio	0.33
Chill	
Youngs modulus (Pa)	115×10^9
Poissons ratio	0.33

*The mechanical properties for the alloy are those for an alloy of similar composition, Al-5.2 wt pct Si (as-cast, diecast condition), and the mechanical properties for the chill material are those for commercially pure grade of Cu. These were obtained from the *Metals Handbook*.[32] The properties are at room temperature.

suggests an additional resistance to heat transfer through an interface containing a gas, which may be significant when considering interfacial gaps of the dimension of the surface roughness (but would not be significant when considering the much larger interfacial gaps that would be created by contraction of the casting away from the chill surface).

The temperature jump coefficient was included by calculating the mean free path of the interfacial gas, assumed to be air, from

$$\lambda = \frac{\mu}{0.499\rho\bar{c}} \quad [3]$$

where μ = dynamic viscosity, ρ = density, and $\bar{c}$ = mean molecular velocity, obtained from

$$\bar{c} = \left(\frac{8kT}{\pi m}\right)^{1/2} \quad [4]$$

where k = Boltzman's constant, T = temperature, and m = the molecular mass of air. The physical properties of air, and other constants used for the determination of the temperature jump coefficient, are given in Table III. The temperature jump coefficient, g, was then calculated from[26,27]

$$\frac{g}{\lambda} = \frac{2-a}{a}\frac{2\gamma}{\gamma+1}\frac{1}{\mathrm{Pr}} \quad [5]$$

where a = the accommodation coefficient (which describes the action of gas molecules in incompletely exchanging thermal energy with a surface), γ = the ratio of specific heats (C_p/C_v), and Pr = the Prandtl number.

The temperature jump coefficient must be evaluated for each surface. In this case, the accommodation coefficient for the chill surface was assumed to be equal to that for the casting surface. The heat-transfer coefficient for the initial contact stage, h_i, was therefore determined from

$$h_i = \frac{k_{\mathrm{air}}}{x + 2g} \quad [6]$$

where k_{air} is the thermal conductivity of the interfacial gas (evaluated at the mean temperature of the chill and casting surfaces) and x is the mean separation of the two surfaces, equal to $R_{z(\Sigma)}/2$. This approach yielded a heat-transfer coefficient for the initial contact stage of about 7 to 8 kW m^{-2} K^{-1}.

B. *The Model of the Deformation of the Initial Casting Skin*

Examination of the surfaces of the Al-7 wt pct Si alloy castings at the chill-casting interface revealed that, although the surface of the chill was plane, the shape of the cast surface

was convex.[16,17,18] Niyama and co-workers had studied this effect[19,20] and showed that a droplet of liquid metal resting on a chilled surface formed a thin solidified skin which then deformed into a parabolic shape. This deformation occurred almost immediately after contact of the liquid metal with the cold surface and once the solidified skin had reached a critical thickness.

A model of the deformation of the initial solidified skin was developed by them[19,20] and was incorporated here. Deformation was assumed to take place once the surface node of the finite difference model of the temperature distribution in the casting reached the solidus temperature of the alloy (850 K). Any possible undercooling was neglected. The temperature gradient within the casting at the time of deformation was calculated from the temperatures of the surface and subsurface nodes of the casting rather than from the temperature of the chill surface, as was originally proposed.[19,20] This gave a predicted curvature of the casting skin that was closer to the measured values obtained in the experiments.

Neglecting the small effect of the critical skin thickness for deformation of the skin, the temperature gradient at the moment of deformation of the casting skin was calculated from

$$G = \frac{T_{\text{subs}} - T_s}{\Delta x} \quad [7]$$

where T_{subs} = the temperature of the subsurface node of the casting, T_s = the temperature of the surface node of the casting, and Δx = the spacing between nodes in the finite difference calculation.

The radius of curvature of the casting surface after deformation was then obtained from

$$R = \frac{1}{\alpha G} \quad [8]$$

where α = the coefficient of linear expansion of pure Al. The displacement of the casting surface due to the deformation, y, at any point on the radius of the interface, r, was then determined from

$$y = \frac{r^2}{2R} \quad [9]$$

For example, the predicted deformation at the circumference of the casting surface was 14.8 μm, 20 pct greater than the measured deformations of the casting surfaces which had a mean value of 12.3 μm.

C. *The Nominal Contact Area between the Casting and the Chill Surfaces*

To determine the area of nominal contact between the curved casting surface and the plane chill surface, the two rough surfaces were considered to overlap to some extent, or to be engaged, at the center of the interface. As the radial distance increased from the center of the interface, the curvature of the casting surface would eventually cause the surfaces to disengage, and a localized gap would form between them. If reference planes for the plane chill surface and the curved casting surface are imagined to be drawn through the midpoints of their respective surface roughness profiles, then the separation between the two planes at the limit of the area of nominal contact, y_{nc}, can be estimated from

$$y_{nc} = R_{z+} - d + \omega \quad [10]$$

The nominal contact area, A_{nc}, was then determined from

$$r_{nc} = 2R(y_{nc})^{0.5} \quad [11]$$

$$A_{nc} = \pi r_{nc}^2 \quad [12]$$

Here, R_{z+} is the arithmetic sum of the R_z values of the two surfaces, d is their separation (obtained as shown in the following section), and ω is the compliance between the two surfaces.

The compliance is defined as the distance points outside the deforming zone approach, *i.e.*, the distance a point in the casting would approach a point in the chill if no deformation occurred between them.[34] In determining the compliance, it was first necessary to determine whether elastic or plastic deformation of the surfaces was to be expected. A criterion for determining the onset of plastic deformation was advanced by Greenwood[28] and Greenwood and Williamson.[29] Elastic deformation only was assumed to have occurred if the compliance did not exceed some critical value, ω_p, given by

$$\omega_p = R(H/E')^2 \quad [13]$$

Here, R is the radius of curvature of the casting skin (Eq. [8]) and E' combines the physical properties of the materials of the two contacting surfaces as follows:

$$\frac{1}{E'} = \frac{(1 - \nu_1^2)}{E_1} + \frac{(1 - \nu_2^2)}{E_2} \quad [14]$$

The term H is the microhardness of the softer material, which in this case was assumed to be the solidifying alloy and which was taken to be approximately 3 times the tensile flow stress.[30]

Temperature-dependant mechanical property data for the model were estimated as follows. Values for the temperature-dependent yield stress of the Al-Si alloy, at low temperatures, were obtained from data for a similar alloy (Al-5.2 wt pct Si),[31] but the yield stress at the solidus temperature of the alloy was estimated from the following considerations. Since alloys begin to develop strength in their mushy phase, as the dendritic solid reaches the point of coherence, their yield strength at the solidus temperature should be low but not zero. For example, Forest and Bercovici[32] measured a tensile strength of greater than 2 MPa at the solidus temperature of an Al-Cu alloy. Therefore, a yield stress at the solidus temperature of 1 MPa was adopted and a temperature-dependant yield stress obtained by interpolation between this and the data for lower temperatures. The Young's modulus (E) of both the alloy and the Cu chill were also assumed to be temperature dependent and to decline linearly to 70 pct of their room temperature values at their respective solidus temperatures.[33] Poissons ratio was assumed to be independent of temperature. This data is shown in Table IV.

The temperature distributions within the casting and the chill obtained from the finite difference calculation at each time-step were used to determine the expansion and contraction and the relative movement of the two surfaces at their interface. At each time-step, their geometric overlap (compliance) was recalculated and compared to the plasticity

criterion (Eq. [13]) for the duration of the solidification and cooling of the casting. This suggested that only elastic deformation at the chill-casting interface was to be expected.

Since the spherical shape of the casting surface was retained after cooling to room temperature, this also suggested that it had experienced negligible plastic deformation during the experiment. The heating of the chill recorded during the experiments showed that the chill would have undergone considerable expansion, but because the casting surface was undeformed, this suggests that the casting was simply pushed away by the expansion of the chill. In the model, the expansion and contraction of the casting and the chill were calculated, and when the force due to the expanding chill matched that due to the metallostatic pressure of the casting, it was assumed that thereafter the casting was pushed away by any further advance. Thus, the load at the casting-chill interface did not exceed that due to the metallostatic pressure of the casting.

Finally, another important assumption was that the surface of the chill remained plane during the cooling of the casting, despite the axial temperature gradient within it.

Having determined that only elastic deformation between the surfaces was to be expected, the compliance between the casting and the chill surfaces was determined as follows. The elastic contact between a convex surface and a plane surface is a classical problem in contact mechanics,[34,35] and the elastic force between them is given by[34]

$$W = (4/3)E'/R^{1/2}\omega^{3/2} \qquad [15]$$

''Hence, the compliance associated with the contact between the plane chill surface and the convex casting surface was determined from''

$$\omega = \left(\frac{3W}{4E'/R^{1/2}}\right)^{2/3} \qquad [16]$$

where W was the load due to the metallostatic pressure of the casting acting over the area of the interface.

D. *The Actual Contact Area between the Casting and the Chill Surfaces within the Nominal Contact Area*

Within the area of nominal contact, the load at the casting-chill interface was supported by contacts between the asperities of the rough casting and chill surfaces. To make the problem more tractable, the two rough surfaces were summed as shown in Eq. [2]. Thus, the problem was made that of a sum rough surface in contact with a plane surface.

Data for the two rough surfaces was obtained using a stylus type surface roughness measuring instrument to obtain values for R_a, R_z, and S_m. The term R_a is the arithmetic mean deviation of the surface profile, R_z is the mean peak-to-valley height measured in the traverse, while S_m is the mean distance between profile peaks (Table I and Figure 2). The mean radius of curvature of the asperity peaks, β, was estimated from values for the mean radius of the asperities, assumed to be $S_{m(\Sigma)}/2$, and a suitable vertical height, assumed to be $R_{z(\Sigma)}/2$

$$\beta = \frac{(S_{m(\Sigma)}/2)^2 + (R_{z(\Sigma)}/2)^2}{R_{z(\Sigma)}/2} \qquad [17]$$

This gave a radius of curvature of the asperities of about 5.6 mm. The area density of asperities was determined from $1/(S^2_{m(\Sigma)})$, and the standard deviation of asperity heights, σ, was assumed to be $R_{a(\Sigma)}$.

Greenwood[28] and Greenwood and Williamson[29] defined a plasticity index, P_i, to determine the likelihood of plastic flow of an asperity:

$$P_i = (\sigma/\beta)^{0.5}\,(E'/H) \qquad [18]$$

specifying 1 as the limit above which the majority of asperities would be expected to deform plastically. In this model, plastic deformation of asperities was assumed to occur as calculated values of the plasticity index for the situation considered here were greatly in excess of 1.

The deformation of the asperities was estimated using a simple ideal plastic model in which the plastically deforming asperity was assumed to be truncated at the surface of contact (*i.e.*, no piling-up of material due to deformation was allowed for). Tabor[36] interpreted ideal plastic deformation such that the pressure at the contact was assumed to be distributed evenly over the contact and to be given by $P = cY$, where Y was the tensile yield stress, and c was some geometry-dependent factor. For hemispherical asperities, $c = 3$.

For ideal plastic deformation, the contact area, A_c, is twice that for elastic deformation:[30]

$$A_c = 2\pi\beta\omega \qquad [19]$$

where ω is now the compliance associated with deformation of the asperity. The contact load, L_c, is therefore given by

$$L_c = cY2\pi\beta\omega \qquad [20]$$

$$= 6Y\pi\beta\omega \qquad [21]$$

The contact radius, r_c, is given by

$$r_c = (2\beta\omega)^{0.5} \qquad [22]$$

From these expressions, the number of asperities in contact and the load they support can be used to calculate their area and, therefore, the heat transfer due to the actual contact between the casting and the chill surfaces.

Following the method of Greenwood and Williamson in their original model,[29] if two surfaces are brought together until they are a distance d apart, there will be contact with an asperity whose height was originally greater than d. The probability of making contact at a given asperity of height z is described by

$$\text{prob}\,(z > d) = \int_d^\infty \Phi(z)dz \qquad [23]$$

where $\Phi(z)$ is some function describing the distribution of asperity heights. If there are N number of asperities on the surface, the expected number of asperities in contact, n_c, will be given by

$$n_c = N\int_d^\infty \Phi(z)dz \qquad [24]$$

For plastic deformation, the area in contact is given by Eq. [19]. Let $\omega = z - d$, then the mean contact area, $\overline{A}_c$, is given by

$$\overline{A}_c = \int_d^\infty 2\pi\beta(z - d)\Phi(z)dz \qquad [25]$$

The total area of all asperities in contact, A_t, is then given by

$$A_t = 2\pi N\beta \int_d^\infty (z - d)\Phi(z)dz \quad [26]$$

and the total load on the asperities in contact, L_t, is given by

$$L_t = 6Y\pi\beta N\int_d^\infty (z - d)\Phi(z)dz \quad [27]$$

If the area density of asperities, η, is given by

$$\eta = \frac{N}{A_{nc}} \quad [28]$$

and a dimensionless separation of the two planes in contact, j, is defined as

$$j = \frac{d}{\sigma} \quad [29]$$

the number of asperities in contact, n_c, is then given by

$$n_c = \eta A_{nc} F_0(j) \quad [30]$$

the total area of the asperities in contact, A_t, is given by

$$A_t = 2\pi\eta A_{nc}\beta\sigma F_1(j) \quad [31]$$

and the total load supported by the asperities in contact, L_t, is

$$L_t = 6Y\pi\beta\eta A_{nc}\sigma F_1(j) \quad [32]$$

where the function $F_n(j)$ is now used to describe the distribution of asperity heights. If an exponential distribution of asperity heights is assumed, the problem is readily solvable[29] having the solution

$$F_n(j) = n!e^{-j} \quad [33]$$

giving the following expressions for n_c, A_t, and L_t

$$n_c = \eta A_{nc} e^{-j} \quad [34]$$

$$A_t = 2\pi\eta A_{nc}\beta\sigma e^{-j} \quad [35]$$

$$L_t = 6\pi Y\beta\eta A_{nc}\sigma e^{-j} \quad [36]$$

If the microscopic load supported by the contacts must equal the load at the interface caused by the metallostatic pressure of the casting, then the dimensionless separation of the two surfaces, j, is determined from Eq. [36]. The number of asperities in contact between the casting and the chill and the area of actual contact can then be determined from Eqs. [34] and [35], respectively.

E. *Calculation of the Heat-Transfer Coefficient*

Once the mean separation of the two planes had been established, then the overall heat-transfer coefficient was obtained as the sum (weighted by area) of the heat-transfer coefficients for the area of nominal contact and the area of the surrounding annulus of local separation. The heat-transfer coefficient for the area of nominal contact was obtained from the sum of the heat-transfer coefficients for the areas in contact and for the intervening voids.

The heat-transfer coefficient for the contact points, h_c, is given by[37,38]

$$h_c = \frac{2k_{hm}n_c/A_{nc}\bar{r}_c}{\phi_{cf}} \quad [37]$$

where k_{hm} is the harmonic mean of the thermal conductivities of the two materials in contact

$$k_{hm} = \frac{2k_1k_2}{k_1 + k_2} \quad [38]$$

$\bar{r}_c$ is the mean contact radius, and ϕ_{cf} is a geometrical factor which models the constriction of the heat flow at the interface through the areas of actual contact. This is given by[30,37,38]

$$\phi_{cf} = (1 - (A_t/A_{nc})^{0.5})^{1.5} \quad [39]$$

The heat-transfer coefficient, h_v, through the void regions of the nominal contact area was estimated from

$$h_v = \frac{k_{\text{air}}}{d/2 + 2g} \quad [40]$$

where $d/2$ is the mean separation of the planes in contact (representing the casting and chill surfaces) determined by the iteration procedure to balance the macroscopically and microscopically supported loads, and k_{air} is the thermal conductivity of the air in the interfacial gap. The dimension of the interfacial gap was increased by including the temperature jump distance, g, evaluated as described in Section A.

The mean separation of the two surfaces in the annulus of local separation surrounding the area of nominal contact, y_a, was determined using the radius of curvature predicted by the Niyama model (Section B). The heat-transfer coefficient describing conduction through the annulus, h_a, was obtained from

$$h_a = \frac{k_{\text{air}}}{y_a + 2g} \quad [41]$$

The overall interfacial heat-transfer coefficient, h_i, was then obtained from

$$h_i = \frac{h_c + h_v}{A_{nc}/A_i} + \frac{h_a}{A_a/A_i} \quad [42]$$

where A_i was the overall area of the casting-chill interface, and the area of the annulus of local separation, A_a, was given by $A_i - A_{nc}$.

IV. RESULTS

Experimentally determined heat-transfer coefficients, obtained during upward solidification of the Al-7 wt pct Si alloy castings, are compared to the predicted heat-transfer coefficient obtained using the model in Figure 3. (The experimentally determined values shown here were also calculated with the thermal conductivity of the bulk liquid increased by a factor of 3.) As can be seen in the figure, a considerable scatter of results was obtained, probably due to uncontrolled variations in the casting procedure used, as is common in these types of experiments. For example, of the four experimentally determined values shown, one experiment resulted in the formation of an air gap at 657 seconds (characterized by a rapid fall in the value of the heat-transfer coefficient), but the remaining three experiments were terminated before an air gap occurred.

Figure 4 shows a comparison between the temperatures measured in the chill, 75 mm from the interface with the casting, with the temperature at the same point calculated by the model. The agreement is reasonable, although the

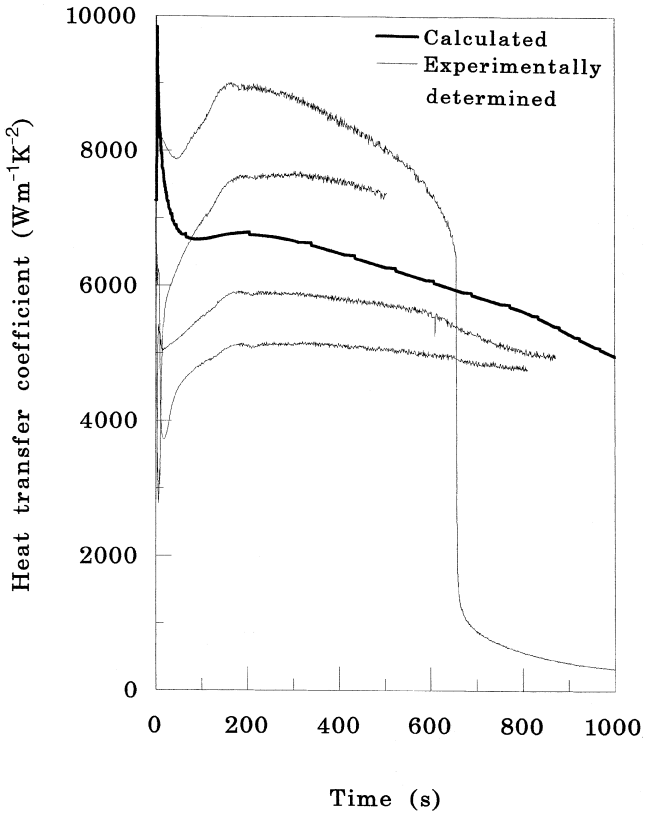

Fig. 3—Graph showing a comparison between the modeled heat-transfer coefficient and experimentally determined values for the unidirectional solidification vertically upward of an Al-7 wt pct Si alloy casting.

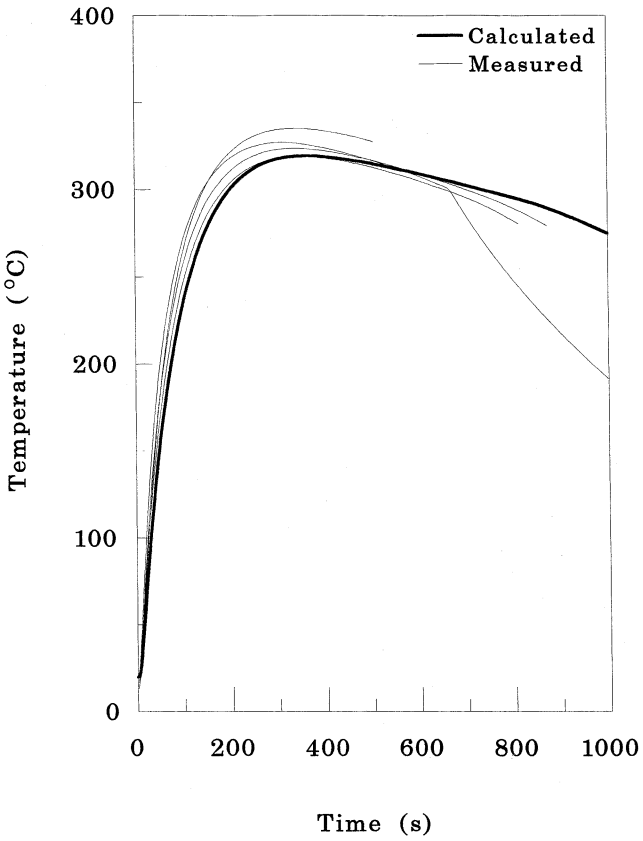

Fig. 4—Comparison of measured and calculated temperatures within the copper chill at a point 75 mm from the casting-chill interface.

calculated temperature is slightly less than the measured ones. Figure 5 shows a similar comparison for the point 75 mm within the casting from the interface. Agreement is good at first, showing the utility of incorporating some provision for the role of heat-transfer due to fluid flow in the bulk liquid of the casting and showing the good agreement obtained by the arbitrary selection of a factor of 3 increase in liquid thermal conductivity. However, thereafter the agreement diverges with the calculated temperatures being greater than the measured temperatures. This is perhaps due to the thermophysical properties of the solid alloy not being precisely known and assumed, for example, to be independent of temperature.

Additional detail about the nature of the casting-chill interface can be extracted from the model. The deformation of the initial solidified skin of the casting was predicted to occur at 3.6 seconds. The radius of the nominal contact area was estimated to be about 8.8 mm or about 50 pct of the total casting-chill interface area. The model suggested that within this area there were slightly more than 70 asperities in contact when solidification of the casting began. The area of actual contact between the casting and the chill surfaces at the beginning of solidification was estimated to be about 0.4 mm^2. This was about 0.17 pct of the nominal contact area or about 0.08 pct of the total area of the casting-chill interface. The mean separation of the two surfaces in the nominal contact area was about 4.3 μm. However, the inclusion of the temperature jump coefficient, g, resulted in an additional gap width of 0.8 μm.

V. DISCUSSION

The approximate agreement obtained between the experimentally determined and modeled heat-transfer coefficients shown in Figure 3, and between the calculated and measured temperatures in the chill and the casting (Figures 4 and 5), suggests that many of the principle mechanisms that govern interfacial heat transfer between the unidirectionally solidified casting and the chill have been recognized and incorporated in the model. A precise agreement cannot be expected because of the wide scatter in the experimentally determined heat-transfer coefficients and because of the many assumptions and estimates involved in the model. Nonetheless, because an important feature of the model was the inclusion of the deformation of the initial solidified skin of the casting, the agreement obtained supports the suggestion that this was a significant factor in the transfer of heat between the casting and the chill.

An overall interfacial heat-transfer coefficient has been modeled because this is how this type of unidirectional solidification experiment is interpreted. However, the basis of the model, of a central contact area surrounded by an annulus in which a local separation had taken place, implies that a macroscopic constriction effect can occur. Heat from the regions of the chill adjacent to the annulus of separation could be conducted through the central nominal contact area at the interface. This is illustrated in Figure 6, which shows examples of the heat-transfer coefficients at 400 seconds in each case. With unidirectional heat transfer assumed, an overall heat-transfer coefficient of about 6480 W m^{-2} K^{-1} was predicted by the model, but the two-dimensional case

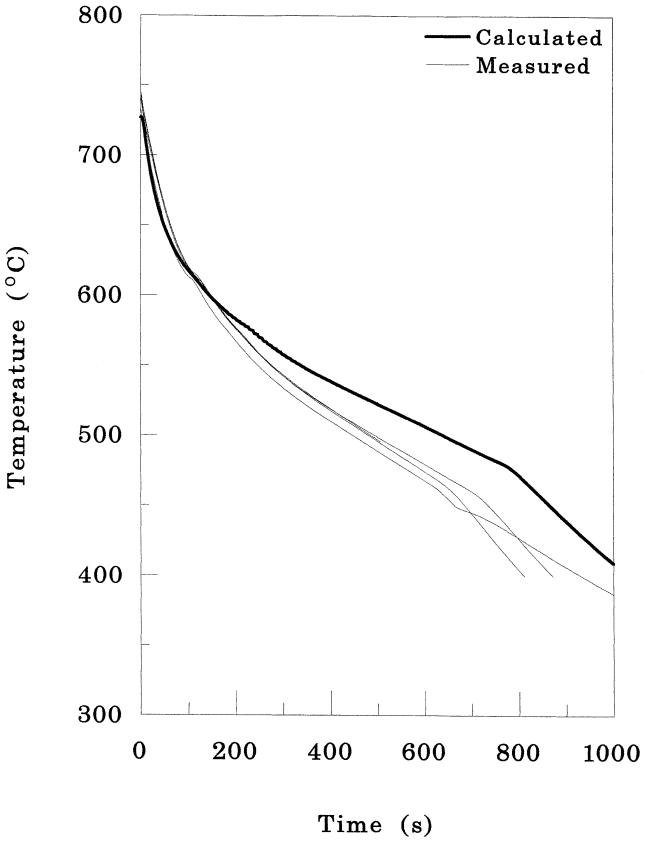

Fig. 5—Comparison of measured and calculated temperatures within the Al-7 wt pct Si alloy casting at a point 75 mm from the casting-chill interface.

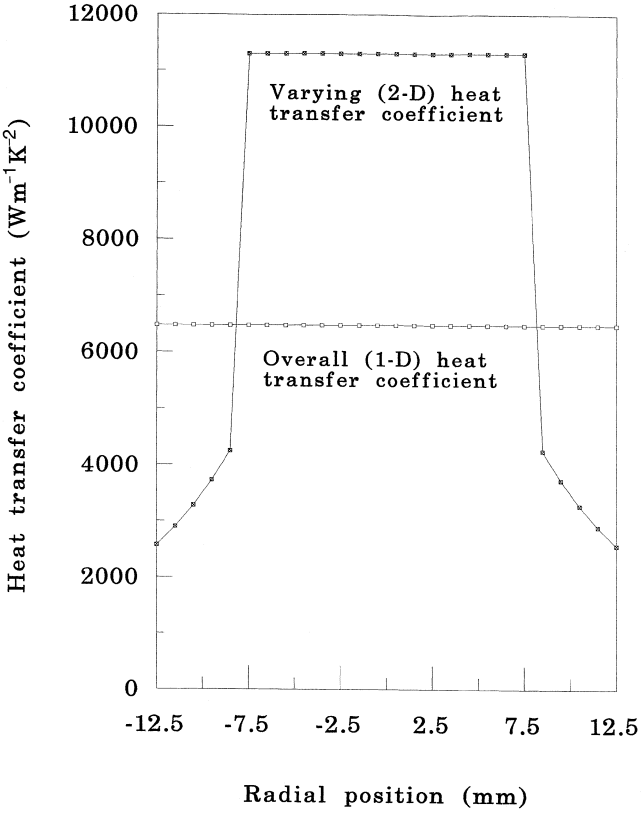

Fig. 6—Graph showing a comparison of the interfacial heat-transfer coefficients with one-dimensional and two-dimensional heat transfer assumed at the casting-chill interface. This graph represent the heat-transfer coefficients occurring 400 s after pouring of the casting.

shows more realistically how the heat-transfer coefficient would vary across the interface. The central region of nominal contact was associated with a heat-transfer coefficient of about 11,300 W m^{-2} K^{-1}, but this declined sharply around the periphery of the interface as the separation of the curved casting surface from the plane chill surface increased with radial distance.

This effect was explored further by calculating the temperature distribution in the casting and the chill assuming one-dimensional heat transfer, using an overall interfacial heat-transfer coefficient, and two-dimensional heat transfer with a heat-transfer coefficient that varied across the interface, as predicted by the model. The resulting calculated temperatures at 5 mm from the interface in the casting and the chill (corresponding to the location of the thermocouples from which the experimentally determined values of the interfacial heat-transfer coefficient were derived) are shown in Figure 7. Assuming a constant heat-transfer coefficient resulted in a slightly greater temperature gradient across the casting-chill interface.

The implications of this were assessed by recalculating overall heat-transfer coefficients using the two different subsurface temperature data shown. This suggested that the (commonly adopted) assumption of one-dimensional heat transfer in the experiment may not be valid in the region where the subsurface thermocouples are usually placed to collect the necessary time-temperature data, *i.e.*, close to the interface. This could lead to an overestimate of the interfacial heat-transfer coefficient which, in the experiment modeled here, may have been as great as 30 pct.

In view of this observation, the comparison of modeled and experimentally determined heat-transfer coefficients shown in Figure 3 are probably not in as good agreement as they appear, although the compared temperatures in Figures 4 and 5 are still valid. Revising the experimentally determined heat-transfer coefficients to lower values would suggest that the model predicted an interfacial heat-transfer coefficient that lay slightly above (rather than within) the scatter of the experimentally obtained results.

The possibility of two-dimensional heat-transfer close to the casting-chill interface has not been considered before and would be an additional source of error in this type of experiment where the heat-transfer coefficient is determined with the assumption of unidirectional heat transfer. The size of this error in any experiment would depend on factors associated with the extent of the deformation of the initial casting skin. These would include the casting radius and the chill temperature, the thermal diffusivity of the metals involved, and the distance of the thermocouples from the casting-chill interface.

The model described here necessarily contained several approximations and assumptions, and its accuracy could be improved by the inclusion of additional detail, as follows. In a practical casting situation, distortion of the casting and the mold due to thermal stress would affect the interfacial pressure between them and, therefore, the heat-transfer coefficient. In this case, distortion of the chill, which was neglected in this work for simplicity, would be expected to

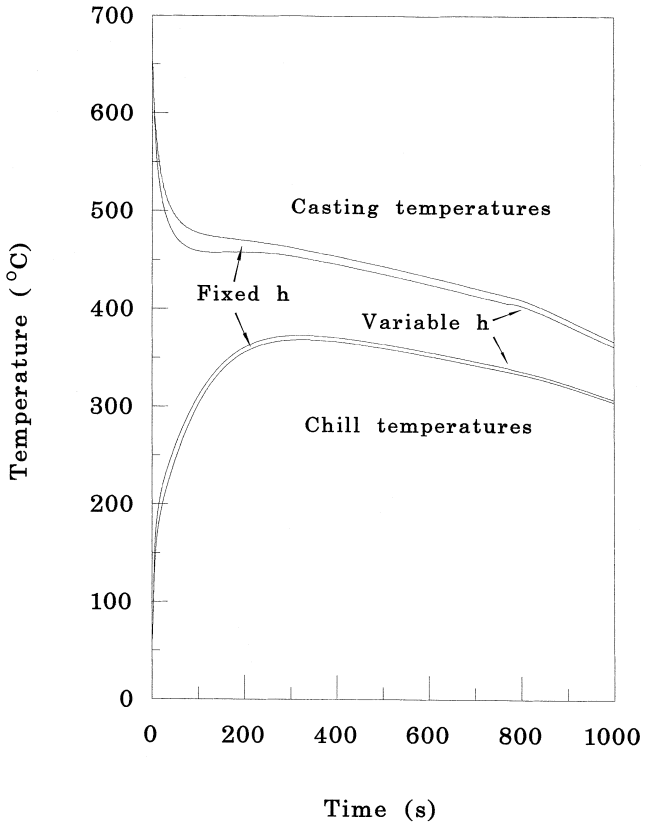

Fig. 7—Graph showing a comparison between the temperatures calculated within the casting and the chill when one-dimensional (fixed *h*) and two-dimensional (variable *h*) heat transfer was assumed at the casting-chill interface. The comparisons are made for a point on the axis of the casting-chill arrangement, 5 mm from their respective interface.

be convex towards the casting and would reduce the modeled heat-transfer coefficient.

Although the refractory fiber tubes in which the castings were made were preheated before use to try to prevent them evolving further gases during the experiment, it is possible that the gas in the interface between the casting and the chill was not solely air, as was assumed. The presence of other gases, such as hydrogen with a much greater thermal conductivity than air, would increase the predicted heat-transfer coefficient.

Several other factors are also poorly known. The model required a knowledge of the mechanical properties of the alloy at temperatures close to its solidus temperature and, as there is little data in the literature concerning the mechanical properties of alloys at high temperatures, these could only be estimated.

Heat transfer during the initial contact stage is poorly understood, and an important factor that was neglected was the extent of the contact area between the cast alloy and the chill surface. The simplifying assumptions made in this model must have led to a considerable underestimate of the heat-transfer coefficient in the first few seconds before the formation of the initial solidified skin of the casting and its deformation.

Also, the effect of any oxide films on the surfaces of the casting and the chill were not taken into account, although only thin films of around 1 μm in thickness were expected, so this assumption would not be expected to introduce serious errors into the model.

The surface roughness data used in the model was an average of values obtained from the measurement of the casting and the chill surfaces in the experiments. However, a considerable scatter in measured values was observed. Furthermore, to simplify the problem, an exponential distribution of asperity heights was assumed. A Gaussian distribution may have been a more accurate representation of the true problem, although this would have required a more complex solution to determine the load supported by the asperities.[29] Furthermore, only plastic deformation of the asperities was assumed in the model, whereas it would have been more realistic to take into account the elastic deformation of the underlying material as well. Finally, such variables as the radius of curvature of the asperity peaks, estimated from the surface roughness measurements, should be determined more accurately.

Nonetheless, despite the limitations and assumptions discussed here, the model described was capable of predicting heat-transfer coefficients that were in approximate agreement with experimentally determined values obtained in the simple unidirectionally solidified castings used. Therefore, this approach may be of considerable assistance in solidification modeling. It could be used to obtain averaged values of an interfacial heat-transfer coefficient, for simplicity, or, for greater accuracy, used to yield locally valid values dependant on the local heat-transfer mechanisms in the interface.

VI. CONCLUSIONS

A model has been developed to predict the interfacial heat-transfer coefficient during unidirectional solidification vertically upward of an Al-7 wt pct Si alloy against a water cooled copper chill. One of the most important features of the model was the incorporation of the deformation of the initial solidified skin of the casting. The agreement obtained between the modeled and experimentally determined values of the interfacial heat-transfer coefficient supports the hypothesis that this was a significant factor in the transfer of heat from the casting to the chill.

ACKNOWLEDGMENTS

The author gratefully acknowledges Federal-Mogul plc for financial support of a Senior Research Fellowship at the Manchester Materials Science Centre during which this research was carried out.

LIST OF SYMBOLS

a	accommodation coefficient
A	area of contact between the casting and the chill
C_p	specific heat capacity (constant pressure)
C_v	specific heat capacity (constant volume)
c	a geometry-dependent factor describing the pressure beneath an indentor
$\bar{c}$	mean molecular velocity
d	mean separation of the casting and the chill
E	Young's modulus
g	temperature jump coefficient
G	temperature gradient

h	heat-transfer coefficient
H	microhardness
j	dimensionless separation of the casting and chill surfaces (d/σ)
k	thermal conductivity
k	Boltzman's constant
L_c	load on the contact area between the casting and the chill
m	molecular mass of a gas
n	number of contacts
N	number of asperities
P_i	plasticity index
Pr	Prandtl number
r	radius of contact area
R	radius of curvature of the casting surface
R_a	arithmetic mean deviation of a surface profile
R_z	mean peak-to-valley height within a surface profile
R_{z+}	arithmetic sum of R_z values for the casting and chill surfaces
S_m	mean distance between profile peaks within a surface profile
W	load at casting-chill interface
x	mean distance between chill and casting surfaces
y	displacement due to deformation of the casting surface
y_a	mean separation between the casting and the chill in the annulus surrounding the area of nominal contact
Y	tensile yield stress
z	asperity height

Subscripts

a	annulus of local separation
c	contact between the casting and the chill surfaces
hm	harmonic mean (thermal conductivities)
i	interface
nc	nominal contact
t	total
v	void

Greek symbols

α	coefficient of thermal expansion
β	radius of curvature of asperity peaks
γ	ratio of specific heats (C_p/C_v)
η	area density of asperities
λ	mean free path of a gas molecule
σ	standard deviation of surface roughness ($\sim R_a$)
Σ	sum surface roughness parameters
μ	dynamic viscosity
ν	Poisson's ratio
$\Phi(Z)$	function describing the distribution of asperity heights
ϕ_{cf}	factor describing heat flow constriction through asperity contacts
ρ	density
ω	compliance (geometrical overlap) between two surfaces

REFERENCES

1. K. Ho and R.D. Pehlke: *AFS Trans.*, 1984, vol. 92, pp. 587-98.
2. K. Ho and R.D. Pehlke: *Metall. Trans. B*, 1985, vol. 16B, pp. 585-94.
3. R.D. Pehlke: *Proc. Modelling of Casting, Welding and Advanced Solidification Processes VII*, M. Cross and J. Campbell, eds. TMS, Warrendale, PA, 1995, pp. 373-80.
4. Y. Nishida, W. Droste, and S. Engler: *Metall. Trans. B*, 1986, vol. 17B, pp. 833-44.
5. M. Trovant and S. Argyropolis: *Proc. Computational Fluid Dynamics and Heat/Mass Transfer Modeling in the Metallurgical Industry*, Montreal, Aug. 24–29, 1996, Canadian Institute of Mining, Montreal, Canada, 1996, pp. 108-22.
6. J. Isaac, G.P. Reddy, and G.K. Sharma: *J. Inst. Eng.: Metall. Mater. Sci. (India)*, 1989, vol. 69, pp. 17-22.
7. H. Huang, J.L. Hill, V.K. Suri, and J.T. Berry: *Proc. Modelling of Casting, Welding and Advanced Solidification Processes V*, TMS, Warrendale, PA, 1991, pp. 65-70.
8. H. Huang, J.L. Hill, and J.T. Berry: *Cast Met.*, 1993, vol. 5, pp. 212-16.
9. H.R. Shahverdi, F. Farhadi, A. Karimitaheri, P. Davami, and K. Asgari: *Cast Met.*, 1994, vol. 6, pp. 231-36.
10. M. Bellet, F. Decultieux, M. Menai, F. Bay, C. Levaillant, J.-L. Chenot, P. Schmidt, and I.L. Svensson: *Metall. Mater. Trans. B*, 1996, vol. 27B, pp. 81-99.
11. O. Jaouen and M. Bellet: *Proc. Modelling of Casting, Welding and Advanced Solidification Processes VIII*, TMS, Warrendale, PA, 1998, pp. 739-46.
12. D.G.R. Sharma and M. Krishnan: *AFS Trans.*, 1991, vol. 99, pp. 429-38.
13. P.M. Mathew, J.W. Devaal, and P.A. Krueger: *Can. Met. Q.*, 1989, vol. 28, pp. 271-83.
14. F. Chiesa: *AFS Trans.*, 1990, vol. 98, pp. 193-200.
15. I.L. Svensson and P. Schmidt: *Cast Met.*, 1993, vol. 6, pp. 127-30.
16. W.D. Griffiths: *Proc. 3rd Pacific Rim Int. Conf. Modelling of Casting and Solidification Processes*, Beijing, Dec. 9–11, 1996, International Academic Publishers, Beijing, 1996, pp. 64-69.
17. W.D. Griffiths: *Metall. Mater. Trans. B*, 1999, vol. 30B, pp. 473-82.
18. R. Kayikci and W.D. Griffiths: *Foundryman*, 1999, vol. 92, pp. 267-73.
19. D. Shu-xin, E. Niyama, K. Anzai, and N. Matsumoto: *Cast Met.*, 1993, vol. 6, pp. 115-20.
20. S.X. Dong, E. Niyama, and K. Anzai: *Iron Steel Inst. Jpn. Int.*, 1995, vol. 35, pp. 730-36.
21. B.G. Thomas and J.T. Parkman: *Proc. Solidification 1998*, TMS, Warrendale, PA, 1998, pp. 509-20.
22. J.P. Holman: *Heat Transfer*, 6th ed., McGraw-Hill Book Company, New York, NY, 1986, pp. 131-206.
23. K. Ho and R.D. Pehlke: *AFS Trans.*, 1983, vol. 91, pp. 689-98.
24. N.A. El-Mahallawy and A.M. Assar: *J. Mater. Sci.*, 1991, vol. 26, pp. 1729-33.
25. *Assessment of Surface Texture, Part 1. Methods and Instrumentation. BS 1134: Part 1: 1988*, British Standards Institution, London, 1988.
26. E.H. Kennard: *Kinetic Theory of Gases*, McGraw-Hill Book Company, New York, NY, 1938, pp. 311-27.
27. M.M. Yovanovich, J.W. DeVaal, and A.H. Hegazy: *Proc. AIAA/ASME 3rd Joint Thermophysics, Fluids, Plasma and Heat Transfer Conf.*, The American Institute of Aeronautics and Astronautics, New York, NY, 1982, pp. 1-7.
28. J.A. Greenwood: *Trans. ASME, J. Lubr. Technol.*, 1967, vol. 89F, pp. 81-91.
29. J.A. Greenwood and J.P.B. Williamson: *Proc. R. Soc. London, A*, 1966, vol. 295, pp. 300-19.
30. B.B. Mikic: *Int. J. Heat Mass Transfer*, 1974, vol. 17, pp. 205-14.
31. *Metals Handbook*, 10th ed., ASM INTERNATIONAL, Materials Park, OH, 1990, vol. 2, pp. 164-65.
32. B. Forest and S. Bercovici: *Proc. Solidification Technology in the Foundry and Cast House*, Coventry, England, Sept. 15–17, 1980, The Metals Society, London, 1980, pp. 607-12.
33. B.M. Drapkin and V.K. Kononenko: *Russ. Metall.*, 1993, vol. 6, pp. 74-77.
34. *Rough Surfaces*, T.R. Thomas, ed., Contact Mechanics, Longman, London, 1982, pp. 168-88.
35. D.J. Whitehouse: *Handbook of Surface Metrology*, IOP Publishing Ltd., Bristol, 1994, pp. 762-75.
36. D. Tabor: *The Hardness of Metals*, Oxford University Press, Oxford, United Kingdom, 1951.
37. M.G. Cooper, B.B. Mikic, and M.M. Yovanovich: *Int. J. Heat Mass Transfer*, 1969, vol. 12, pp. 279-99.
38. M.R. Sridhar and M.M. Yovanovich: *J. Thermophys. Heat Transfer*, 1994, vol. 8, pp. 633-40.